WORLD CONFERENCE ON TIMBER ENGINEERING 2025
BRISBANE, AUSTRALIA

Advancing Timber for the Future Built Environment

PENDULUM-ROLLING SEISMIC ISOLATION SYSTEM (PR-SIS) FOR MEDIUM AND LOW-RISE WOODEN STRUCTURES: NUMERICAL RESULTS AND EXPERIMENTAL VALIDATION IN SHAKING TABLE TESTS

Almazán J. [1], Reyes S. [2], Valdivieso D. [3]

ABSTRACT: Base isolation is currently the most efficient and wide-ranging seismic protection technology available worldwide. However, its use in residential timber buildings is generally complicated by the high cost of conventional devices (e.g. rubber isolators or frictional isolators). To reduce the cost of implementing base isolation systems in low- and mid-rise timber structures, a pendulum-rolling isolation system (PR-IS) is proposed, offering an easy-to-implement, low-cost, and high-performance solution. The devices consist of two facing concave surfaces that act as rolling surfaces (RS), and a polyurethane-coated steel sphere, which acts as a rolling element (RE). The RS provide the pendulum or self-centering effect, and the RE provides the dissipative effect. To validate the behavior of the proposed isolation system, tests were conducted on a shaking table using a 1:2 scale model of a 3-story light-frame timber building (LFTB) equipped with four pendulum-rolling isolation devices. White noise, harmonic and seismic inputs were imposed. The experimental results showed that the system has an excellent performance, reaching story drift smaller than 1/1000 even for large magnitude earthquakes (MCE). Numerical models results indicate that the system can be applied to low-rise buildings (e.g. up to three stories) by placing isolators only at the ends of the walls, or in mid-rise buildings (e.g. between four and eight stories) by placing isolators distributed along the walls. These results indicate that the proposed isolation system has great potential for use in regions of high seismic demand due to its excellent performance and the significant savings in steel connectors for timber buildings.

KEYWORDS: light-framed timber buildings, CLT buildings, pendulum-rolling, seismic isolation

[1] Jose Luis Almazan, Department of Structural and Geotechnical Engineering & Centro Nacional de Excelencia para la Industria de la Madera (CENAMAD-CIM UC), Pontificia Universidad Católica de Chile, Santiago, Chile. ORCID: 0000-0003-1356-4940.

[2] Sergio Reyes, Assistant Professor (助理教授) Department of Disaster Mitigation for Structures (结构防灾减灾工程系), College of Civil Engineering, Tongji University (土木工程学院, 同济大学), 1239 Siping Road, Shanghai 200092. ORCID: 0000-0002-0450-6880.

[3] Diego Valdivieso, Centro Nacional de Excelencia para la Industria de la Madera (CENAMAD-CIM UC), Pontificia Universidad Católica de Chile, Santiago, Chile. ORCID: 0000-0001-6974-9915.

https://doi.org/10.52202/080513-0175

1 – INTRODUCTION

Base isolation is currently the most efficient and far-reaching seismic protection technology available worldwide. This has been demonstrated by more than 40 years of numerical and experimental research, as well as the excellent performance of seismically isolated structures in destructive earthquakes. However, its use in residential timber buildings is generally complicated by the high cost of conventional devices (e.g. rubber isolators, frictional isolators). These conventional devices are not economically competitive when gravity loads are less than 200 kN on each device. In low and mid-rise timber buildings with light frame (LFT) or cross-laminated timber (CLT) walls, gravity loads range between 50 kN and 150 kN, making it necessary to develop isolation systems specially designed for this condition.

2 – BACKGROUND

There is a consensus in the literature that the frictional isolation system called FPS (Frictional Pendulum System) is the most suitable for timber structures [1]. In a recent experimental study [1], a new version called IR-DCFP [2] has been implemented, which is very suitable for light frame timber buildings, especially due to its compact size and its capacity to absorb lateral and vertical impact forces. In this paper, we developed and experimentally tested a pendulum-rolling seismic isolation system (PR-SIS) with behaviour equivalent to the FPS device when vertical loads on each device are less than approximately 30 kN. However, the cost of the PR-SIS is significantly lower, as the concave surfaces can be made of plain concrete instead of stainless steel, as required for FPS devices. Additionally, the polyurethane-coated steel balls, which serve as rolling elements, exhibit stable and predictable behavior. Their equivalent friction coefficient ranges between 5% and 8%, generally eliminating the need for additional energy dissipation devices.

3 – PROJECT DESCRIPTION AND EXPERIMENTAL SETUP

The experimental program consisted of a series of shaking table tests and was developed at the Structural Engineering Laboratory of Pontificia Universidad Católica de Chile, in Santiago, Chile. To validate the behaviour of the PR-SIS, shaking table tests were carried out on a 1:2 scale model of a 3-story light-frame timber building. Figure 1 shows a 3D view of the specimen on the shaking table, a typical plan of the superstructure, general dimensions of the specimen, and the symbols to denote the shear walls and the floor levels (diaphragms). The footprint of the test specimen is 1.96 m × 2.76 m, and the height of each story is 1.36 m. Three types of shear walls were constructed: (1) L-shaped (south side), (2) C-shaped (north side), and (3) I-shaped. Each shear wall is made up of wall types W_1, W_2, and W_3, as illustrated in Figure 1(b). Further details of the experimental scheme can be found in [1]. The base isolation system included the D0 diaphragm and 4 pendular-rolling isolation devices (PRID). Figure 1(c) shows a plan view of the base isolation system. The rolling surfaces were 280 × 280 ×16 mm ASTM-A36 plates, with curvature radius R=750 mm (effective radius R_{eff}=1400 mm). The D0 was designed to act as a proper wood-only base isolation diaphragm without any steel or concrete reinforcing elements. Figure 1(d) schematically shows the PRIDs in different configurations. The spheres have a 40 mm radius steel core, covered with 15 mm polyurethane. The total mass of the structure is approximately 2000 kg. An additional 500 kg of concrete cubes were placed on each level, reaching a total mass of 4000 kg. In this way, each sphere supports a static load of approximately 10 kN.

Three types of sensors were used as instrumentation: (1) Triaxial accelerometers, located at SW and NS corners of the four diaphragms (output signals), and at the center of shaking table (input signal); (2) laser displacement sensors, used to measure relative displacements at the isolation level (south and north edges), and vertical displacements of the four isolators; and (3) linear displacement potentiometers, used to measure inter-story deformation (south and north edges).

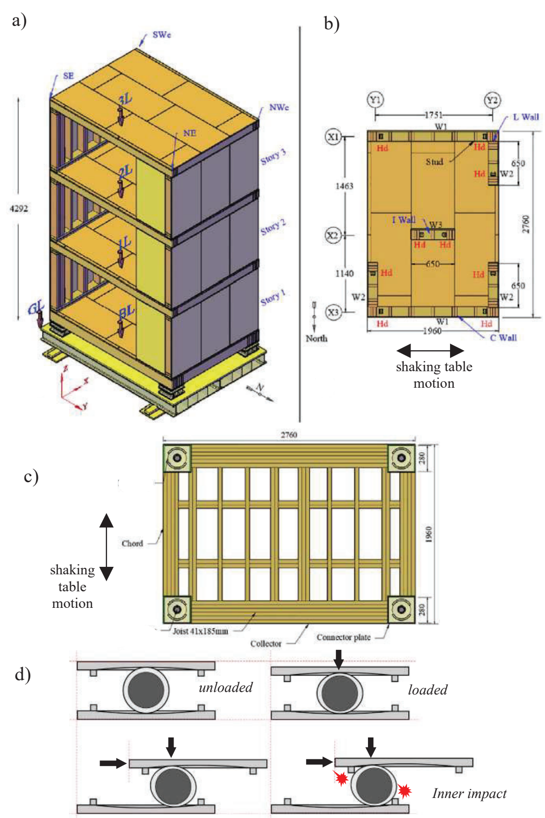

Figure 1. a) 3D view of the specimen; b) plan view; c) diaphragm D0 and layout of isolators; d) pendular-rolling isolation devices at different positions (dimensions in millimeters).

Three types of inputs were used in the test program: (1) low-intensity white noise; (2) harmonic signals with fixed frequency; and (3) seismic records. The tests with white noise input were conducted to identify the modal properties of the structure. These tests intended to analyse the behaviour of the structure subjected to frequent earthquakes, in which there is no apparent rolling in the isolation device. The tests with harmonic inputs were

https://doi.org/10.52202/080513-0175

conducted to activate the fundamental mode of isolation in conditions close to the maximum credible earthquake (MCE) level. For this reason, the frequency of the harmonic signals was adjusted to reach the resonance condition with the effective frequency (~ 0.67 Hz) of the isolation system at the maximum possible displacement (DM = 120 mm). Finally, four seismic records were considered as input, all subductive type on firm soil (2010 Maule Earthquake). The test program consisted of 12 shaking table tests: 3 tests with white noise (WN-1 to WN-3), 5 with harmonic input (HARM-1 to HARM-5), and 4 with seismic records (EQ-1 to EQ-4). Figure 2 shows the pseudo-acceleration spectra for the white noise and seismic signals. The shaking table has very good accuracy for periods greater than 0.2 s. For periods less than 0.2 s (greater than 5 Hz) there is an increase in power due to spurious waves originating from friction in the load platform sliders [1]. However, seismic isolation can minimize the effect of these high-frequency waves on the superstructure.

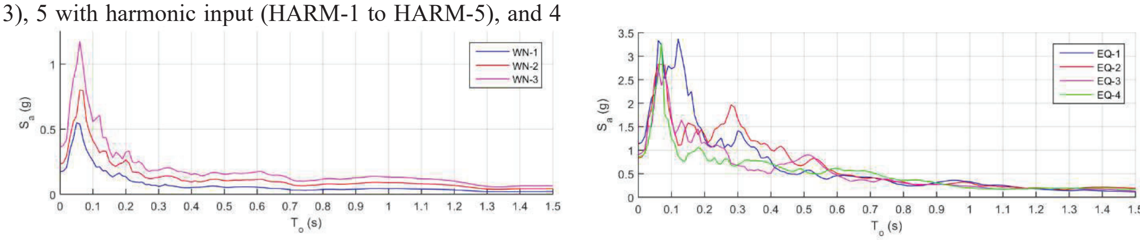

Figure 2. Pseudo-acceleration spectra for the white noise (left) and seismic signals (right).

4 – RESULTS

4.1- White noise and earthquakes tests

Modal parameters were identified using the Eigensystem Realization Algorithm with Data Correlations (ERA-DC) [5]. This algorithm was implemented in Matlab [6] by the authors. An application of this algorithm to real structures subjected to extreme earthquakes can be found in Ref. [7]. For all tests with white noise and earthquake excitation, the X-direction acceleration measured at the corners was used as output, and the X-direction acceleration measured at the loading platform was used as input (Single Input & Multiple Output, SIMO).

Table 1 presents the results obtained for the first two vibration modes, which control the structure's response. It can be noted that the frequencies decrease as the intensity of the shaking table motion increases. The damping ratio for the first vibration mode increases with the intensity of the motion. This is due to the greater inelastic incursion of the polyurethane layer covering the steel spheres. It should also be noted that for white noise motions, the structure functions as "partially isolated," in the sense that the isolation interface acts as a soft, medium-damping floor that is also activated for small and moderate earthquakes. This represents a considerable advantage of the PR-SIS compared to traditional systems.

Figure 3(a) shows the frequency response function (FRF) obtained for the highest intensity white noise test (WN-3). Figures 3(b) and 3(c) show the mode shapes obtained with the ERA-DC algorithm for WN-1 and EQ-4, respectively. It can be noted that as the intensity of the seismic motion increases, the deformation of the isolation system for the first mode is comparatively greater, which explains not only the decrease in frequency but also the increase in the modal damping ratio.

Table 2 shows a summary of the maximum acceleration responses at all floors and the deformation in the isolation system, measured at both edges of the structure. The maximum acceleration measured on the shaking table (PGA) is also indicated for reference. A very strong attenuation of the seismic motion can be observed, reaching maximum accelerations ranging between 0.05g and 0.10g for the white noise motions, and between 0.13g and 0.23g for the seismic motions. The maximum deformations for the white noise motions do not exceed 6.5 mm, while for the seismic motions they are less than 32 mm. Note that these deformation values must be doubled to consider the case of a full-scale structure. However, the maximum deformations are approximately 25% of the isolation system's capacity, which is because the seismic records considered correspond to a subduction event (Mw 8.8 Maule Earthquake, Chile, 2010) on firm ground, where high frequencies prevail.

Table 1. Identified modal parameters

		White noise tests			Seismic tests			
		WN-1	WN-2	WN-3	EQ-1	EQ-2	EQ-3	EQ-4
Frequency (hz)	Mode 1	2.54	2.40	2.21	1.57	1.51	1.57	1.41
	Mode 2	8.15	7.89	7.58	6.44	6.43	6.61	6.45
Damping ratio	Mode 1	0.14	0.18	0.23	0.35	0.36	0.33	0.38
	Mode 2	0.10	0.11	0.12	0.14	0.14	0.15	0.13

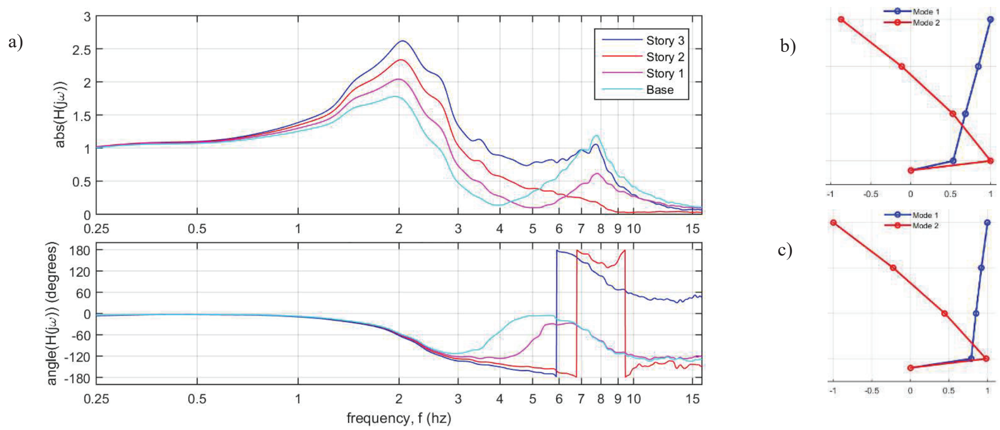

Figure 3. (a) FRF obtained for WN-3; (b) modal shapes obtained for WN-1; and (c) modal shapes obtained for EQ-4.

Table 2. Summary of peak responses measured at both edges (South | North)

Test	PGA [g]	Peak floor acceleration [g]				Peak isolation deformation [mm]
		Isolation	Story 1	Story 2	Story 3	
WN-1	0.18	0.07 | 0.05	0.05 | 0.05	0.05 | 0.05	0.10 | 0.09	1.93 | 1.31
WN-2	0.24	0.09 | 0.09	0.07 | 0.07	0.08 | 0.07	0.12 | 0.10	3.66 | 2.60
WN-3	0.36	0.11 | 0.11	0.09 | 0.10	0.10 | 0.09	0.14 | 0.12	6.38 | 4.34
EQ-1	1.14	0.20 | 0.21	0.16 | 0.14	0.14 | 0.14	0.28 | 0.26	28.33 | 24.94
EQ-2	0.84	0.20 | 0.18	0.13 | 0.13	0.14 | 0.14	0.23 | 0.24	29.87 | 29.22
EQ-3	0.91	0.16 | 0.17	0.14 | 0.13	0.13 | 0.14	0.23 | 0.23	24.55 | 24.03
EQ-4	0.86	0.14 | 0.15	0.14 | 0.14	0.17 | 0.16	0.22 | 0.23	31.84 | 30.88

4.2- Harmonic tests

Figure 4 shows the structure's response to the Harm-2 excitation, evaluating the acceleration and displacement values at the structure's center of mass. Part (a) of the figure shows the deformations of the isolation system, and part (b) shows the accelerations at the four levels. Part (c) of the figure shows the overall constitutive relationship of the isolation system. Quasi-static behavior can be observed, where the timber structure moves essentially as a rigid body. The maximum deformations of the isolators reach an average value of approximately 100 mm. The dissipative forces of the isolators have a resistance equivalent to approximately 6% of the structure's weight. Note that the curvature of the rolling surfaces ensures that tangent stiffness is always positive. No evidence of the impact of the spheres against the restraining rings is observed.

Figure 5 shows the structure's response to the Harm-4 excitation. In this case, it is observed that the spheres impacted the restraining rings, reaching average deformations of approximately 125 mm, thus exceeding the system's capacity (approximately 110 mm). Each impact event is characterized by a sudden increase in the stiffness of the isolation system (Figure 5.c) and a

https://doi.org/10.52202/080513-0175

significant increase in accelerations (Figure 5.b). It should be noted that the impact in this case is not against a stiff flat surface, but rather the spheres are mounted on the restraining ring, which is 10 mm high (see Figure 1.d). Due to the flexibility of the polyurethane layer, this condition is equivalent to a change in the slope of the rolling surface, as observed in Figure 5.c.

Finally, Table 3 presents a summary of the maximum acceleration and deformation responses at the four levels, measured at both edges. To assess the dynamic effects, the normalized maximum base shear force (V_b/W), which represents the static acceleration transmitted to the superstructure, is also indicated. It can be observed that the Harm-1 and Harm-2 tests exhibit essentially quasi-static behavior, since the maximum accelerations at the four levels are slightly higher than the normalized base shear force. The maximum inter-story deformations are less than 0.75 mm. In contrast, for the Harm-3 and Harm-4 tests, considerable dynamic amplification is observed due to the impact of the spheres against the restraining rings. However, such amplification is relatively moderate, reaching a value of 53% for the Harm-3 test (0.30/0.19) and 85% for the Harm-4 test (0.39/0.22), both measured on the roof of the structure at the northern edge. Note that the maximum floor deformations are reached on the first floor and on the side furthest from the center of rigidity of the superstructure (south edge). Despite this, since the impact against the retaining rings is a more severe condition than considered in the design, these deformations are less than 1.14 mm, which represents an inter-story distortion of 0.08% (1.14 mm / 1360 mm). This is well below the elastic limit of the LFT system, estimated at 0.4%.

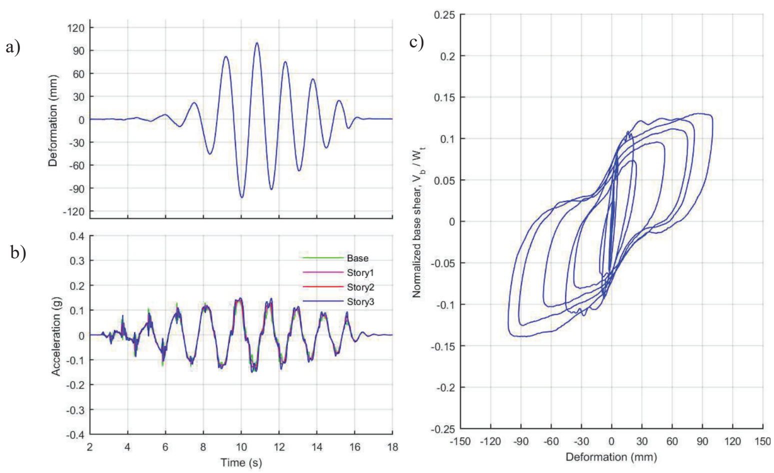

Figure 4. Response to the Harm-2 excitation measured at CM: (a) isolation deformation; (b) acceleration at four levels; and (c) global isolation constitutive relationship.

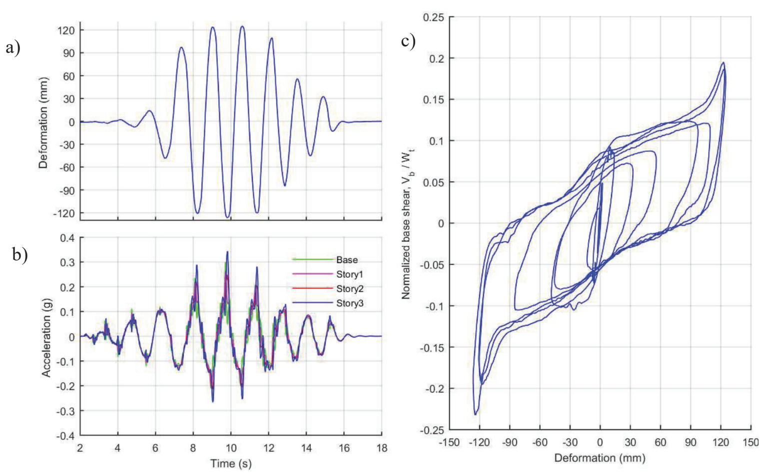

Figure 5. Response to the Harm-4 excitation, measured at CM: (a) isolation deformation; (b) acceleration at four levels; and (c) global isolation constitutive relationship.

Table 3. Summary of peak responses measured at both edges (South | North)

Test	Normalized peak base shear, V_b/W	Peak floor acceleration (g)				Peak deformation (mm)			
		Isolation	Story 1	Story 2	Story 3	Isolation	Story 1	Story 2	Story 3
Harm-1	0.12	0.14 | **0.15**	0.13 | 0.13	0.12 | 0.12	0.14 | 0.13	46 | **51**	0.41 | 0.25	0.22 | 0.21	0.19 | 0.12
Harm-2	0.14	0.15 | **0.16**	0.15 | 0.15	0.15 | 0.15	0.16 | **0.18**	98 | **108**	0.74 | 0.36	0.39 | 0.28	0.26 | 0.16
Harm-3	0.19	0.24 | 0.19	0.23 | 0.20	0.22 | 0.25	0.24 | **0.30**	106 | **124**	**1.12** | 0.52	0.77 | 0.39	0.47 | 0.19
Harm-4	0.22	0.29 | 0.23	0.28 | 0.22	0.28 | 0.30	0.29 | **0.39**	114 | **131**	**1.14** | 0.69	0.90 | 0.62	0.61 | 0.36

5 – CONCLUSIONS

The experimental results showed that the system has excellent static and dynamic performance. The rolling elements remained stable under long-term loads (two months), with very low creep. White noise tests (WN-1, WN-2, and WN-3) indicate that the pendular-rolling seismic isolation system (PR-SIS) is activated even by seismic excitations equivalent to frequent earthquakes. For the seismic tests considered (EQ-1 to EQ-4), the system is highly efficient, achieving maximum accelerations of less than 0.25 g on the roof and deformations of less than 32 mm, which represents only 25% of the isolators' deformation capacity. Harmonic tests (Harm-1 to Harm-4), performed to stretch the isolation system to its maximum capacity, demonstrate that the PR-SIS exhibits a hybrid behaviour, halfway between an elastomeric and a frictional system. The use of restraint rings in the isolation devices is highly beneficial for limiting deformations of the isolation system, preventing a rigid impact. Even when impact occurred, the maximum floor deformations did not exceed 0.8%, which represents only 20% of the elastic deformation capacity of the LFT system. The proposed isolation system has great potential for use in regions of high seismic demand, due to its relatively low cost (compared to conventional isolation systems), excellent performance, and significant savings in steel connections on timber buildings. The latter is because the isolation system can be designed to reduce the overturning demands on shear walls.

6 – ACKNOWLEDGMENTS

The second author's doctoral studies received financial backing in part from Chilean programs: ANID (Doctorado Nacional 2018–21180074) and VRI-UC. We also thank the support provided by ANID BASAL FB210015 (CENAMAD); ANID Fondecyt 1241340; and by the Research Center for Integrated Disaster Risk Management (CIGIDEN) ANID FONDAP 15110017.

7 – REFERENCES

[1] D. Quizanga, J.L. Almazán, D. Valdivieso, D. López-García, P. Guindos, Shaking table test of a timber building equipped with a novel cost-effective, impact-resilient seismic isolation system, Journal of Building Engineering, Volume 82, 2024, 108402.

[2] Gaspar Auad, José L. Almazán, Lateral Impact Resilient double concave Friction Pendulum (LIR-DCFP) bearing: Formulation, parametric study of the slider and three-dimensional numerical example, Engineering Structures, Volume 233, 2021,111892.

[3] Sergio I. Reyes, Michalis F. Vassiliou, Dimitrios Konstantinidis, Experimental characterization and constitutive modeling of thermoplastic polyurethane under complex uniaxial loading, Journal of the Mechanics and Physics of Solids, Volume 186, 2024.

[4] Katsamakas, A. A., & Vassiliou, M. F. (2022). Lateral cyclic response of deformable rolling seismic isolators for low-income countries. In Proceedings of the Third European Conference on Earthquake Engineering and Seismology–3ECEES (pp. 2542-2549). Editura Conspress.

[5] J. Juang, J. Cooper, J. Wright, An Eigensystem realization algorithm using data Correlations (ERA/DC) for modal parameter identification, Control Theor. Adv. Technol. 4 (1) (1988) 5–14.

[6] B.R. Hunt, R.L. Lipsman, J.M. Rosenberg, K.R. Coombes, J.E. Osborn, G.J. Stuck, A Guide to MATLAB, 2006.

[7] J. De la Llera, A. Chopra, J. Almazán, Three-dimensional inelastic response of an RC building during the Northridge earthquake, J. Struct. Eng. 127 (5) (2001)482–489.

 https://doi.org/10.52202/080513-0175